Analysis on Decode-and-Forward Two-Path Relay Networks: When and How to Cooperate

Hao Lu, Peilin Hong, and Kaiping Xue, *Member, IEEE*

***Abstract*—Two-path relay networks can be deployed to achieve full-rate transmissions. In this paper, we introduce stable throughput analysis into decode-and-forward (DF) two-path relay networks. We establish the queueing model and take outage probabilities into consideration to characterize the packet-level cooperation and derive the closed-form stable throughput region. Based on the stable throughput region, we also propose a power-allocation scheme between the source node and relays to maximize the achievable packet rate. The maximal achievable packet rate determines the admission control of certain cooperation (i.e., when to cooperate) under a specific interrelay interference (IRI) cancellation technique. The power allocation is utilized to illustrate how to cooperate between the source node and relays. Three IRI responses are considered, and the system behaviors under various circumstances are presented through simulations.**

***Index Terms*—Interrelay interference (IRI), power allocation, stable throughput region, two-path relay.**

I. Introduction

The cooperative communication technique has attracted a lot of interests in recent years since it can improve the network coverage and diversity performance. Due to the half-duplex nature of a relay (i.e., a node can either "transmit" or "receive" at any time instant in the same channel), conventional one-way relay networks require two time slots for the relay to receive the signal and then forward it, respectively [1]. Thus, a cooperative scheme named two-path successive relay was introduced to overcome such bandwidth inefficiency [2], [3]. As shown in Fig. 1, at each time slot, source node S transmits its packet to one of the relays, and the other relay simultaneously forwards the signal received from S at the previous slot. As a consequence, the source node has access to the channel within each slot, named full-rate transmission. Meanwhile, the two-path relay has introduced interrelay interference (IRI), whereas the receiving relay suffers the interference from the transmitting relay, marked as red bold arrows in Fig. 1. Diverse schemes were proposed to deal with the IRI [4]–[7]. In our previous works [8], [9], we exploited physical-layer network coding and complex field network coding (CFNC) to cancel IRI.

Since all existing works are focused on IRI cancellation techniques, they lack analysis and discussions on the following aspects for two-path relay networks. First, only the symbol error rate or the bit error rate is derived in those papers, whereas the achievable data rate is related to the end-to-end packet error rate, which is characterized by outage probability. Second, no power allocation is performed in their studies since power allocation plays a significant role in system performance in conventional relay-based networks. The system has to decide whether QoS requirements (e.g., data rate) can be satisfied under such cooperation and how to cooperate to achieve better system behavior. These decisions depend on the appropriate power-allocation scheme.

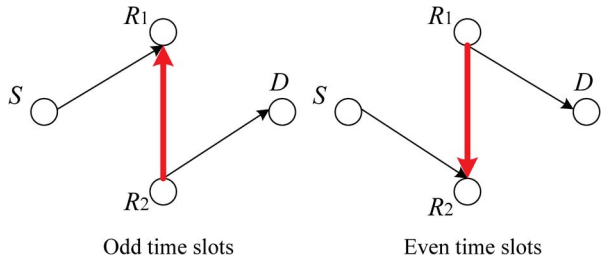

Fig. 1. Two-path relay model.

In this paper, we first propose a cross-layer model for decode-and-forward (DF) two-path relay networks. In AF relay systems, both the noise and the IRI are amplified and forwarded to the destination, resulting in performance degradation and complicated detections. Thus, DF relays are considered in our paper. The "cross-layer" represents that we introduce queueing stability (upper layer) into analysis to characterize packet-level cooperative transmissions, together with the outage probability in the physical layer. Based on this model, we present the stable throughput region of the source node, where the stable throughput region is defined as the set of all arrival rate vectors (in packets/slot) to the source such that all queues in the network remain bounded, which has been applied to the analysis in one-way relay networks and cognitive radio [10], [11]. Subsequently, to determine when and how to cooperate, we perform power allocation to maximize the achievable throughput (i.e., data rate) subjected to stable throughput constraints. Furthermore, the analysis and simulations of three scenarios are derived and compared, respectively, in our paper: 1) the case with no IRI cancellation technique, 2) the IRI cancellation scheme proposed in [5], and 3) the CFNC-based IRI cancellation scheme in our previous work [9].

The rest of this paper is organized as follows. Section II depicts the system model, and the stable throughput region is derived. The theoretical analysis on power allocation under three scenarios is given in Section III, and simulation results are presented in Section IV. Finally, Section V summarizes this paper.

Notations: λ is the packet arrival rate; μ is the packet service rate; ρ is the outage probability; $\mathcal{CN}(0,\sigma^2)$ is the circular symmetric complex Gaussian distribution with zero mean and variance σ^2; $\exp(1/\sigma^2)$ is the exponential distribution with mean σ^2; $\Pr\{\mathrm{A}\}$ is the probability of event A; $\mathbb{E}$ is the mathematical expectation; $\angle X$ is the phase of X; and x^* is the conjugate of x.

II. System Model and Stable Throughput Region

Here, we will present the DF two-path relay model and the packet-level cooperation strategy with queueing process. Subsequently, the closed-form stable throughput region of our model is derived.

A. Networks and Links

As shown in Fig. 1, this paper considers a two-path relay network that consists of one source node S, one destination node D, and two

Manuscript received February 10, 2015; revised May 11, 2015; accepted July 3, 2015. Date of publication July 13, 2015; date of current version July 14, 2016. This work was supported in part by the National Science Foundation of China under Grant 61379129 and Grant 61170231 and in part by the National High-Tech Research and Development Plan of China (863 Program) under Grant 2014AA01A706. The review of this paper was coordinated by Dr. X. Huang.

The authors are with the Wireless Information Network Laboratory, Department of Electronic Engineering and Information Science, University of Science and Technology of China, Hefei 230027, China (e-mail: lluhao@mail.ustc.edu.cn; plhong@ustc.edu.cn; kpxue@ustc.edu.cn).

Color versions of one or more of the figures in this paper are available online at http://ieeexplore.ieee.org.

Digital Object Identifier 10.1109/TVT.2015.2455497

DF relays R_1 and R_2. Each node is equipped with a single antenna and operates in half-duplex mode. The relays have no data to send. As the same assumptions in [5]–[8], we ignore a direct link between the source and the destination due to long distance. The packets can only be transmitted through source–relay–destination. The transmit power of the source node is P_s, and the transmit power of each relay is P_r. Since the source and the relay will transmit packets simultaneously within the same spectrum, they can be treated as a single transmitter by other nodes in the network. Thus, the sum of source's and relay's transmit power should meet the power constraint for conventional one-hop noncooperation transmissions to prevent severe interference. Hence, in this paper, we consider $P_s + P_r \leq P_{\text{th}}$. Such constraint is also deployed by [12] and conventional one-way relay networks when performing power allocation. We let G_{ij} represent the channel gain between transmitting node i and receiving node j ($i \in \{s, 1, 2\}$ and $j \in \{1, 2, d\}$), where $1, 2$ stand for the relay nodes R_1, R_2. Channel gains between R_1 and R_2 satisfy channel reciprocity (i.e., $G_{12} = G_{21}$). The instantaneous channel gain accounts for the path loss and Rayleigh fading, which is expressed as

$$G_{ij} = L_{ij}^{-\alpha} \cdot |h_{ij}|^2 \tag{1}$$

where L_{ij} is the distance between i and j with path-loss exponent α. In addition, $h_{ij} \sim \mathcal{CN}(0, 1)$ is modeled as zero-mean complex Gaussian random variables with unit variance. Thus, we have $G_{ij} \sim \exp(1/\sigma_{ij}^2)$, where $\sigma_{ij}^2 = L_{ij}^{-\alpha}$. Under normal circumstances, each receiver is aware of channel state information (CSI), i.e., h_{1d}, h_{2d} are known at D and relay R_i is aware of h_{si}, h_{12} ($i \in \{1, 2\}$). All channel coefficients remain constant within one packet time and vary independently from packet to packet. The corresponding channel noise at each receiver is assumed to be complex additive white Gaussian noise with variance N_0.

B. Packet-Level Cooperation and Queueing Model

We consider slot-by-slot transmissions where 1 s is divided into T time slots, where we let the duration time of one slot be one packet transmission period. Packets are generated at the source node with average rate λ_s (packets/slot). The cooperative transmission is performed as follows. We assume that at each odd slot, the source node transmits the packet to R_1, whereas R_2 simultaneously forwards the packet to the destination. At each even slot, the source's packet is received by R_2, whereas R_1 forwards the packet in its queue. If the corresponding relay successfully decodes the packet, it broadcasts an acknowledgement (ACK) to the source; thus, the packet exits the source's queue while this relay will keep the packet and take the responsibility to forward it; otherwise, the packet stays in the source's queue, waiting to be retransmitted. Meanwhile, if the packet is not successfully decoded at the destination, the packet will stay in the relay's queue and be retransmitted within the next corresponding time slot. All ACKs are instantaneous and error-free.

Our objective is to maximize the achievable throughput (i.e., maximal λ_s). Thus, the source should keep transmitting either a new coming packet or a retransmission packet within each time slot. However, in fact, although the source node can keep transmitting within each slot, IRI does not always exist. For example, when R_1 fails to decode the current packet, retransmission is performed by the source, and R_1 has a positive probability to keep silent within the next slot, i.e., no IRI to R_2's receiving. This is why we introduce the queueing model at each transmitter to characterize the transmission, unlike conventional research on the physical layer where the IRI is always assumed to be existent.

According to Loynes' Theorem [13], which states that if the arrival and service processes of a queue are strictly stationary and ergodic, the queue is stable if and only if the average arrival rate is strictly less than the average service rate. Assuming no packet dropouts at the transmitter (i.e., enough cache for arrived packets), the average service rate of the source node is $\mu_s = (\mu_{s1} + \mu_{s2})/2$ (packets/slot), where μ_{s1} and μ_{s2} are the average service rates of $S{-}R_1$ and $S{-}R_2$ links, respectively. Service rate is equal to the probability that one packet is successfully decoded at receiver. Hence, we have

$$\begin{aligned}\mu_{s1} &= \Pr\{Q_2 = 0\}(1 - \rho_{s1}) + \Pr\{Q_2 > 0\}\left(1 - \rho_{s1}^{(I)}\right) \\ &= \left(1 - \frac{\lambda_2}{\mu_2}\right)(1 - \rho_{s1}) + \frac{\lambda_2}{\mu_2}\left(1 - \rho_{s1}^{(I)}\right) \end{aligned} \tag{2}$$

$$\begin{aligned}\mu_{s2} &= \Pr\{Q_1 = 0\}(1 - \rho_{s2}) + \Pr\{Q_1 > 0\}\left(1 - \rho_{s2}^{(I)}\right) \\ &= \left(1 - \frac{\lambda_1}{\mu_1}\right)(1 - \rho_{s2}) + \frac{\lambda_1}{\mu_1}\left(1 - \rho_{s2}^{(I)}\right) \end{aligned} \tag{3}$$

where Q_1 and Q_2 are the lengths of the queue at R_1 and R_2, respectively. $Q_i = 0$ represents that there is no packet in queue i and R_i keeps silence (i.e., no IRI within this slot). Based on Little's law [14], the probability of nontransmission in a G/G/1 queue is $(1 - (\text{arrival rate}/\text{service rate}))$. Hence, λ_1 and μ_1 are the average packet arrival rate and the service rate at relay R_1, whereas λ_2 and μ_2 correspond to R_2. The first term in (2) denotes that no packet is transmitted by R_2, i.e., no IRI to R_1. The second term characterizes the IRI case. Likewise, it is the same for μ_{s2} in (3). Thus, ρ_{s1} stands for the outage probability of the $S{-}R_1$ link when IRI is not existent, whereas $\rho_{s1}^{(I)}$ characterizes the outage probability of the IRI case. Without IRI, the outage probabilities ρ_{s1} and ρ_{s2} can be expressed as

$$\rho_{s1} = \Pr\left\{W \log\left(1 + \frac{P_s G_{s1}}{N_0}\right) < R\right\} = 1 - e^{-\frac{N_0 \eta}{P_s \sigma_{s1}^2}} \tag{4}$$

$$\rho_{s2} = \Pr\left\{W \log\left(1 + \frac{P_s G_{s2}}{N_0}\right) < R\right\} = 1 - e^{-\frac{N_0 \eta}{P_s \sigma_{s2}^2}} \tag{5}$$

where

$$\eta = 2^{\frac{R}{W}} - 1. \tag{6}$$

W is the bandwidth. Channel gain $G_{s1} \sim \exp(1/\sigma_{s1}^2)$, and $G_{s2} \sim \exp(1/\sigma_{s2}^2)$. Assuming one packet contains K $bits$, we have $R = KT$. The calculations of $\rho_{s1}^{(I)}$ and $\rho_{s2}^{(I)}$ vary based on different IRI cancellation techniques, which will be detailed in the next section.

While the source node keeps transmitting within each slot, the average packet arrival rates at relays are the same as the service rates of the source node, i.e.,

$$\lambda_1 = \mu_{s1} \tag{7}$$

$$\lambda_2 = \mu_{s2}. \tag{8}$$

Meanwhile, the average service rates at relays depend on relay–destination links, characterized as

$$\mu_1 = 1 - \rho_{1d} = 1 - \Pr\left\{W \log\left(1 + \frac{P_r G_{1d}}{N_0}\right) < R\right\} = e^{-\frac{N_0 \eta}{P_r \sigma_{1d}^2}} \tag{9}$$

$$\mu_2 = 1 - \rho_{2d} = 1 - \Pr\left\{W \log\left(1 + \frac{P_r G_{2d}}{N_0}\right) < R\right\} = e^{-\frac{N_0 \eta}{P_r \sigma_{2d}^2}} \tag{10}$$

where $G_{1d} \sim \exp(1/\sigma_{1d}^2)$, $G_{2d} \sim \exp(1/\sigma_{2d}^2)$, and ρ_{1d} and ρ_{2d} are the outage probabilities of $R_1{-}D$ and $R_2{-}D$ link, respectively.

C. Stable Throughput Region

Based on (2), (3), and (7)–(10), we have

$$\mu_{s1}=\frac{(1-\rho_{s1})(1-\rho_{2d})-(1-\rho_{s2})\left(\rho_{s1}^{(I)}-\rho_{s1}\right)}{(1-\rho_{1d})(1-\rho_{2d})-\left(\rho_{s1}^{(I)}-\rho_{s1}\right)\left(\rho_{s2}^{(I)}-\rho_{s2}\right)}(1-\rho_{1d}) \tag{11}$$

$$\mu_{s2}=\frac{(1-\rho_{s2})(1-\rho_{1d})-(1-\rho_{s1})\left(\rho_{s2}^{(I)}-\rho_{s2}\right)}{(1-\rho_{1d})(1-\rho_{2d})-\left(\rho_{s1}^{(I)}-\rho_{s1}\right)\left(\rho_{s2}^{(I)}-\rho_{s2}\right)}(1-\rho_{2d}). \tag{12}$$

The stability of the entire network requires the stability of each send queue, i.e., $\{\lambda_s<\mu_s,\ \lambda_1<\mu_1,\ \lambda_2<\mu_2\}$. Subsequently, we present the results with respect to the stable throughput region.

Theorem 1: In a DF two-path relay network, the stable throughput region of the source–destination connection is characterized by

$$\mathcal{R}=\left\{\begin{array}{l}\text{(a) } \lambda_s<\frac{\mu_{s1}+\mu_{s2}}{2}\\ \text{(b) } \frac{(1-\rho_{s1})(1-\rho_{2d})-(1-\rho_{s2})\left(\rho_{s1}^{(I)}-\rho_{s1}\right)}{(1-\rho_{1d})(1-\rho_{2d})-\left(\rho_{s1}^{(I)}-\rho_{s1}\right)\left(\rho_{s2}^{(I)}-\rho_{s2}\right)}<1\\ \text{(c) } \frac{(1-\rho_{s2})(1-\rho_{1d})-(1-\rho_{s1})\left(\rho_{s2}^{(I)}-\rho_{s2}\right)}{(1-\rho_{1d})(1-\rho_{2d})-\left(\rho_{s1}^{(I)}-\rho_{s1}\right)\left(\rho_{s2}^{(I)}-\rho_{s2}\right)}<1\end{array}\right\} \tag{13}$$

where (13b) and (13c) are based on $\lambda_1=\mu_{s1}<\mu_1$ and $\lambda_2=\mu_{s2}<\mu_2$, respectively.

III. Power Allocation

In conventional one-way relay networks, power allocation plays a significant role in determining system performance. It helps to decide whether the QoS requirement can be satisfied through cooperation and how to cooperate to achieve maximal data rate. Therefore, we model a generalized power-allocation problem for a DF two-path relay system based on our stable throughput constraints and derive its solutions based on different IRI responses.

Our objective is to maximize the achievable packet arrival rate at source node, i.e., maximizing the service rate μ_s. Thus, the optimization problem is characterized as

$$\lambda_s^*=\max_{P_s,P_r}\ \frac{\mu_{s1}+\mu_{s2}}{2} \tag{14a}$$

$$\text{s.t.}\quad \lambda_1\le\mu_1 \tag{14b}$$

$$\lambda_2\le\mu_2 \tag{14c}$$

$$P_s+P_r\le P_{\text{th}} \tag{14d}$$

where (14b) and (14c) correspond to the stable throughput constraint. Before resolving this problem, we first introduce the following lemma.

Lemma 1: Suppose t_1 and t_2 are independent exponentially distributed random variables with means σ_1^2 and σ_2^2. Then, we have

$$\Pr\left\{\frac{t_1}{t_2+a}<b\right\}=1-\frac{\sigma_1^2}{\sigma_1^2+b\sigma_2^2}e^{-\frac{ab}{\sigma_1^2}}. \tag{15}$$

Proof:

$$\begin{aligned}\Pr\left\{\frac{t_1}{t_2+a}<b\right\}&=\mathbb{E}|_{t_2}\left\{\Pr\left\{t_1<b(t_2+a)|t_2\right\}\right\}\\&=\int_0^\infty\frac{1}{\sigma_2^2}e^{-\frac{t_2}{\sigma_2^2}}\int_0^{b(t_2+a)}\frac{1}{\sigma_1^2}e^{-\frac{t_1}{\sigma_1^2}}dt_1dt_2\\&=1-\frac{\sigma_1^2}{\sigma_1^2+b\sigma_2^2}e^{-\frac{ab}{\sigma_1^2}}.\end{aligned} \tag{16}$$

■

Different IRI cancellation strategies result in different λ_s^*. Subsequently, we consider three scenarios mentioned in Section I and deduce the optimal λ_s^*, respectively. In the following derivations, we add subscripts "A,B,C" to the notations to distinguish different scenarios.

A. Decoding Without IRI Cancellation

In the conventional way without any IRI response, the signals from the source node are directly detected by the relay, with symbols from the other relay being treated as interference. Thus, the outage probabilities are calculated based on the signal-to-interference-plus-noise ratio, which are expressed as

$$\begin{aligned}\rho_{s1,A}^{(I)}&=\Pr\left\{W\log\left(1+\frac{P_sG_{s1}}{P_rG_{12}+N_0}\right)<R\right\}\\&=1-\frac{P_s\sigma_{s1}^2}{P_s\sigma_{s1}^2+\eta P_r\sigma_{12}^2}e^{-\frac{N_0\eta}{P_s\sigma_{s1}^2}}\end{aligned} \tag{17}$$

$$\begin{aligned}\rho_{s2,A}^{(I)}&=\Pr\left\{W\log\left(1+\frac{P_sG_{s2}}{P_rG_{12}+N_0}\right)<R\right\}\\&=1-\frac{P_s\sigma_{s2}^2}{P_s\sigma_{s2}^2+\eta P_r\sigma_{12}^2}e^{-\frac{N_0\eta}{P_s\sigma_{s2}^2}}\end{aligned} \tag{18}$$

where $G_{12}\sim\exp(1/\sigma_{12}^2)$, and subscript "$A$" represents the case without IRI cancellation. The calculations are based on **Lemma 1**. Based on expressions of the outage probabilities of all links, λ_i,μ_i are only determined by (P_s,P_r) if W,R,N_0,σ_{ij}^2 are given ($i\in\{s,1,2\},j\in\{1,2,d\}$). Thus, the packet arrival rates and service rates can be expressed as $\lambda_{i,A}(P_s,P_r)$ and $\mu_{i,A}(P_r)$.

The original problem (14) is nonconvex and is intractable in its original form. To obtain $\lambda_{s,A}^*$, we introduce the following proposition.

Proposition 1: When the maximal available packet arrival rate $\lambda_{s,A}^*$ is achieved, the sum of the corresponding transmit powers of the source and the relay, which are represented by $P_{s,A}^*$ and $P_{r,A}^*$, respectively, is equal to P_{th}. In addition, for at least one of the two relays, the packet arrival rate is the same as its service rate. Mathematically, we have

$$P_{s,A}^*+P_{r,A}^*=P_{\text{th}} \tag{19}$$

$$\lambda_{1,A}\left(P_{s,A}^*,P_{r,A}^*\right)=\mu_{1,A}\left(P_{r,A}^*\right)$$

$$\text{or}\quad \lambda_{2,A}\left(P_{s,A}^*,P_{r,A}^*\right)=\mu_{2,A}\left(P_{r,A}^*\right). \tag{20}$$

Proof: The proof of this proposition is provided in the Appendix. ■

Therefore, we can obtain $\lambda_{s,A}^*$ through two steps.

Step 1: Replacing P_r with $P_{\text{th}}-P_s$, function $f_A(P_s)$ is defined as

$$\begin{aligned}f_A(P_s)&=\mu_{1,A}(P_{\text{th}}-P_s)-\lambda_{1,A}(P_s,P_{\text{th}}-P_s)\\&\overset{(a)}{=}(1-\rho_{1d})-\frac{(1-\rho_{s1})(1-\rho_{2d})-(1-\rho_{s2})\left(\rho_{s1,A}^{(I)}-\rho_{s1}\right)(1-\rho_{1d})}{(1-\rho_{1d})(1-\rho_{2d})-\left(\rho_{s1,A}^{(I)}-\rho_{s1}\right)\left(\rho_{s2,A}^{(I)}-\rho_{s2}\right)}\end{aligned} \tag{21}$$

where (a) is based on the expressions on μ_1 and λ_1 in (7), (9), and (11). All the outage probabilities in (21) are calculated by (4), (5), (9), (10), (17), or (18). Then according to $f_A(P_s)=0$, we can obtain P_s. Furthermore, in order to obtain a closed-form expression on P_s, we utilize the first-order Taylor expansion of exponential function. We replace $e^{-N_0\eta/P_i\sigma_{ij}^2}$ with $(1-(N_0\eta/P_i\sigma_{ij}^2))$ in (4), (5), (9), (10), (17), and (18) and then substitute them into (21). After simplifications, $f_A(P_s)=0$ is given as

$$P_s{}^4+a_1P_s{}^3+a_2P_s{}^2+a_3P_s+a_4=0 \tag{22}$$

where

$$V = \frac{1}{\sigma_{12}^2\sigma_{1d}^2\sigma_{s1}^2\sigma_{s2}^2} \tag{23a}$$

$$a_1 = V\cdot\left(\sigma_{12}^2\sigma_{1d}^2\left(N_0\eta\left(\sigma_{s1}^2+\sigma_{s2}^2\right)+2P_{\rm th}\sigma_{s1}^2\sigma_{s2}^2\right) -N_0\left(\sigma_{s1}^2+\sigma_{1d}^2\right)\left(\sigma_{s1}^2-\eta\sigma_{12}^2\right)\left(\sigma_{s2}^2-\eta\sigma_{12}^2\right)\right) \tag{23b}$$

$$a_2 = V\cdot\left(\sigma_{12}^2\sigma_{1d}^2\left(N_0^2\eta^2+2P_{\rm th}N_0\eta\left(\sigma_{s1}^2+\sigma_{s2}^2\right)+P_{\rm th}^2\sigma_{s1}^2\sigma_{s2}^2\right) +P_{\rm th}N_0\sigma_{1d}^2\left(\sigma_{s1}^2-\eta\sigma_{12}^2\right)\left(\sigma_{s2}^2-\eta\sigma_{12}^2\right)\right) - P_{\rm th}N_0\eta\left(\sigma_{12}^2\sigma_{s1}^2+\sigma_{12}^2\sigma_{s2}^2-2\eta\sigma_{12}^4\right)\left(\sigma_{s1}^2+\sigma_{1d}^2\right) \tag{23c}$$

$$a_3 = V\cdot\left(P_{\rm th}^2N_0\eta\left(\sigma_{12}^2\sigma_{s1}^2+\sigma_{12}^2\sigma_{s2}^2-2\eta\sigma_{12}^4\right) -\sigma_{12}^2\sigma_{1d}^2\left(P_{\rm th}^2N_0\eta\left(\sigma_{s1}^2+\sigma_{s2}^2\right)+2P_{\rm th}N_0^2\eta^2\right) -P_{\rm th}^2N_0\eta^2\sigma_{12}^4\left(\sigma_{s1}^2+\sigma_{1d}^2\right)\right) \tag{23d}$$

$$a_4 = V\cdot\left(P_{\rm th}^2N_0\eta^2\sigma_{12}^2\sigma_{1d}^2\left(N_0+P_{\rm th}\sigma_{12}^2\right)\right) \tag{23e}$$

where all the parameters in (23a)–(23e) are the same as those defined in previous expressions or derivations. The Ferrari's formula [15] can be utilized to obtain the closed-form roots of (22) (a quartic polynomial equation). Subsequently, the feasible solution set for P_s is given by

$$\mathcal{A}_{\rm Step1} = \{P_s | f_A(P_s)=0,\ \angle P_s = 0,\ 0<P_s<P_{\rm th}, \lambda_{2,A}(P_s, P_{\rm th}-P_s) \le \mu_{2,A}(P_{\rm th}-P_s)\} \tag{24}$$

where $\angle P_s = 0$ denotes that the phase of P_s is 0 (i.e., P_s is a real number).

Step 2: We define another function $g_A(P_s) = \mu_{2,A}(P_{\rm th}-P_s) - \lambda_{2,A}(P_s, P_{\rm th}-P_s)$. Likewise, let $g_A(P_s)=0$, we obtain the feasible solution set

$$\mathcal{A}_{\rm Step2} = \{P_s | g_A(P_s)=0,\ \angle P_s = 0,\ 0<P_s<P_{\rm th}, f_A(P_s)\ge 0\}. \tag{25}$$

Finally, the optimal transmit power of the source node is

$$P_{s,A}^* = \underset{P_s\in\mathcal{A}_{\rm Step1}\bigcup\mathcal{A}_{\rm Step2}}{\arg\max}\ \frac{\mu_{s1}+\mu_{s2}}{2} \tag{26}$$

and $P_{r,A}^* = P_{\rm th} - P_{s,A}^*$.

B. IRI Cancellation Scheme in [5]

In [5], the orthogonality of the real and imaginary parts of the symbol was exploited to distinguish the information and interference at relays. For example, within each odd slot, the source only transmits the real component of its modulated symbols, whereas the symbols forwarded by R_2 only contain their imaginary component. As a result, the receiver can separate the information from interference through simply extracting the real or imaginary phase of the received signal. We use subscript B to stand for the case in [5]. Thus, $\rho_{s1,B}$, $\rho_{s1,B}^{(I)}$, $\rho_{s2,B}$, and $\rho_{s2,B}^{(I)}$ are given by

$$\rho_{s1,B} = \rho_{s1,B}^{(I)} = \Pr\left\{\frac{W}{2}\log\left(1+\frac{P_sG_{s1}}{N_0}\right)<R\right\} = 1-e^{-\frac{N_0\left(2^{\frac{2R}{W}}-1\right)}{P_s\sigma_{s1}^2}} \tag{27}$$

$$\rho_{s2,B} = \rho_{s2,B}^{(I)} = \Pr\left\{\frac{W}{2}\log\left(1+\frac{P_sG_{s2}}{N_0}\right)<R\right\} = 1-e^{-\frac{N_0\left(2^{\frac{2R}{W}}-1\right)}{P_s\sigma_{s2}^2}}. \tag{28}$$

For relay–destination links, we have

$$\rho_{1d,B} = \Pr\left\{\frac{W}{2}\log\left(1+\frac{P_rG_{1d}}{N_0}\right)<R\right\} = 1-e^{-\frac{N_0\left(2^{\frac{2R}{W}}-1\right)}{P_r\sigma_{1d}^2}} \tag{29}$$

$$\rho_{2d,B} = \Pr\left\{\frac{W}{2}\log\left(1+\frac{P_rG_{2d}}{N_0}\right)<R\right\} = 1-e^{-\frac{N_0\left(2^{\frac{2R}{W}}-1\right)}{P_r\sigma_{2d}^2}}. \tag{30}$$

It can be easily proved that $P_{s,B}^*$ and $P_{r,B}^*$ still satisfy the properties in **Proposition 1**.

Since $\rho_{s1,B} = \rho_{s1,B}^{(I)}$ and $\rho_{s2,B} = \rho_{s2,B}^{(I)}$, $\lambda_{1,B}(P_{s,B}, P_{r,B}) = \mu_{1,B}(P_{r,B})$ is equivalent to $\rho_{s1,B} = \rho_{1d,B}$, i.e.,

$$P_{s,B} = \frac{\sigma_{1d}^2}{\sigma_{s1}^2+\sigma_{1d}^2}P_{\rm th}. \tag{31}$$

Meanwhile, according to $\lambda_{2,B}(P'_{s,B}, P'_{r,B}) = \mu_{1,B}(P'_{r,B})$, we have

$$P'_{s,B} = \frac{\sigma_{2d}^2}{\sigma_{s2}^2+\sigma_{2d}^2}P_{\rm th}. \tag{32}$$

Therefore, $P_{s,B}^*$ can be expressed as

$$P_{s,B}^* = \min\left\{\frac{\sigma_{1d}^2}{\sigma_{s1}^2+\sigma_{1d}^2}P_{\rm th}, \frac{\sigma_{2d}^2}{\sigma_{s2}^2+\sigma_{2d}^2}P_{\rm th}\right\} \tag{33}$$

and $P_{r,B}^* = P_{\rm th} - P_{s,B}^*$.

C. IRI Cancellation Based on CFNC

In our previous works [9], CFNC-based IRI cancellation technique requires that the symbols sent by the source node are multiplied by precoding factor θ_1, whereas the symbols transmitted by relays are multiplied by θ_2. Precoding factors satisfy that $|\theta_1| = |\theta_2| = 1$ and $\theta_1x_s + \theta_2x_r \ne \theta_1x'_s + \theta_2x'_r$ if $(x_s, x_r) \ne (x'_s, x'_r)$, where x_s and x_r are the symbols sent by the source node and one of the relays, respectively. The design of precoding factors is given in [9] and will not be detailed in this paper. Within those slots without IRI, the outage probabilities are the same as those without precoding factors due to all the modulated symbols only going through the same phase rotation. Thus, $\rho_{s1,C}$, $\rho_{s2,C}$, $\rho_{1d,C}$, and $\rho_{2d,C}$ are the same as those in (4), (5), (9), and (10), respectively. If both the source and one of the relays simultaneously transmit packet within the slot, the received signal at the other relay i is expressed as

$$y_i = \sqrt{P_sL_{si}^{-\alpha}}h_{si}\theta_1x_s + \sqrt{P_rL_{12}^{-\alpha}}h_{12}\theta_2x_r + \omega_i \tag{34}$$

where ω_i is the noise at relay i. Maximum-likelihood detection is performed at relay i as

$$(x_s, x_r) = \arg\min_{x_s,x_r}\left\|y_i - \left(\sqrt{P_sL_{si}^{-\alpha}}h_{si}\theta_1x_s + \sqrt{P_rL_{12}^{-\alpha}}h_{12}\theta_2x_r\right)\right\|^2. \tag{35}$$

Since it is difficult to calculate the outage probability of the source–relay link, we utilize the upper bounds of $\rho_{s1,C}^{(I)}$ and $\rho_{s2,C}^{(I)}$ to obtain a suboptimal solution. The upper bounds corresponds to the case that outage event occurs unless both the packets from the source and the other relay can be decoded. Since $|\theta_1| = |\theta_2| = |x_s| = |x_r| = 1$, we

TABLE I
SIMULATION PARAMETERS

Parameters	Value
Bandwidth (W)	180kHz
Packets/slot	1000
Bits/Packet	1024
Path-loss Exponent (α)	4
Small-scale Fading	Rayleigh fading
Power Constraint (P_{th})	23 dBm
Noise Power	-174 dBm/Hz
L_{sd}	300m

have $\sqrt{P_s L_{si}^{-\alpha}} h_{si}\theta_1 x_s \sim \mathcal{CN}(0, P_s\sigma_{si}^2)$ and $\sqrt{P_r L_{12}^{-\alpha}} h_{12}\theta_2 x_r \sim \mathcal{CN}(0, P_r\sigma_{12}^2)$. The two terms are independent of each other. Thus, we have $(\sqrt{P_s L_{si}^{-\alpha}} h_{si}\theta_1 x_s + \sqrt{P_r L_{12}^{-\alpha}} h_{12}\theta_2 x_r) \sim \mathcal{CN}(0, P_s\sigma_{si}^2 + P_r\sigma_{12}^2)$. This multiaccess channel can be equivalently treated as a single channel. We let $P_{\text{sig.},i} = (\sqrt{P_s L_{si}^{-\alpha}} h_{si}\theta_1 x_s + \sqrt{P_r L_{12}^{-\alpha}}\, h_{12}\,\theta_2 x_r)^* \cdot (\sqrt{P_s L_{si}^{-\alpha}}\, h_{si}\theta_1 x_s + \sqrt{P_r L_{12}^{-\alpha}}\, h_{12}\theta_2 x_r)$, where $P_{\text{sig.},i}$ is the received signal power at relay R_i and $P_{\text{sig.},i} \sim \exp(1/(P_s\sigma_{si}^2 + P_r\sigma_{12}^2))$. Then, the outage probability of the $S-R_i$ link $\rho_{si,C}^{(I)}$ $(i \in \{1, 2\})$ is calculated by

$$\rho_{si,C}^{(I)} = \Pr\left\{W \log\left(1+\frac{P_{\text{sig.},i}}{N_0}\right) < 2R\right\} = 1 - e^{-\frac{N_0\left(2^{\frac{2R}{W}}-1\right)}{P_s\sigma_{si}^2 + P_r\sigma_{12}^2}} \quad (36)$$

where the factor "2" before R stands for that the symbols from the source and the other relay are jointly detected. Subsequently, the same as the derivations in Section III-A, the optimal solution can be achieved after two steps' calculation based on *Proposition 1*. The first-order approximation of the Taylor expansion can be utilized to obtain closed-form expressions, which are similar to scenario A. The derivations will not be detailed here, and the results are given in simulations.

D. Discussions

Before a two-path relay connection is established, we first determine whether such cooperation can satisfy the stable throughput constraint with λ_s at the source node. Only when $\lambda_s < \lambda_{s,k}^*$, the connection can be established with IRI response k ($k \in \{A, B, C\}$). A larger stable throughput region requires a complicated IRI cancellation technique. For example, a CFNC-based scheme leads to the best system behavior at the cost of the most complicated calculations. When IRI response k is selected, then $P_{s,k}^*$ and $P_{r,k}^*$ indicate how to cooperate.

IV. SIMULATIONS

Through simulations, this section provides the achievable packet rates with different IRI cancellation techniques under various scenarios. According to the Third-Generation Partnership Project (3GPP) evaluation guideline [16], some primary simulation parameters are presented in Table I, where L_{sd} is the distance between the source and the destination.

First, the relays are configured in the middle area between the source and the destination (i.e., $L_{si} \approx L_{id}$). The distance between the two relays is $L_{12} = 100$ m. The results are presented in Fig. 2. The notations "A," "B," and "C" correspond to different IRI responses discussed in Section III-A–C, respectively. For the scenario without the IRI cancellation strategy (A), the packet rate could hardly exceed 0.5 due to severe IRI. For scenario B, owning to the orthogonality of the in-phase and quadrature-phase components of the modulated symbols, the achievable packet rate is larger than that of scenario A. However, it

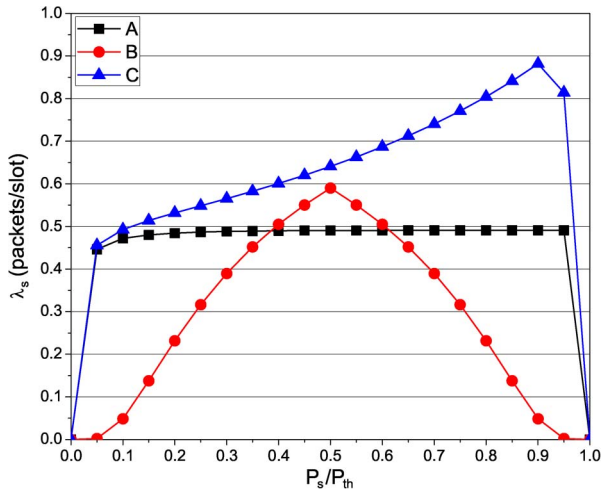

Fig. 2. Achievable packet rates based on different IRI cancellation schemes. $L_{12} = 100$ m.

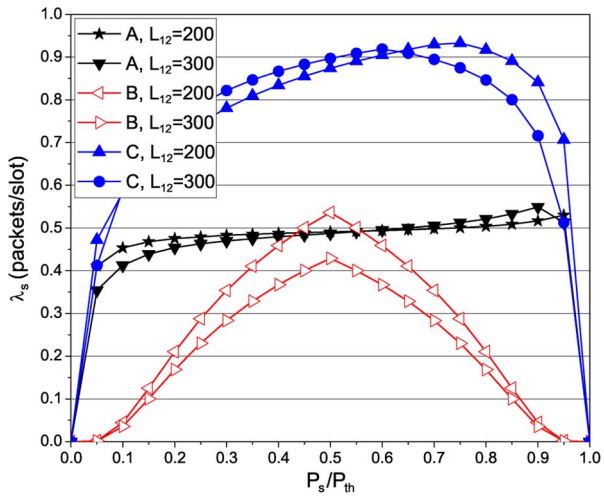

Fig. 3. Achievable packet rates based on different IRI cancellation schemes with various distance protection between relay nodes.

suffers from the loss of modulation degree. When CFNC is adopted to deal with the IRI (C), the IRI is treated as part of the signal to jointly decode the packets. Within the slots without IRI, the precoding factor will not affect the detection of the source's symbols. Thus, high packet rates can be obtained.

In Fig. 3, we vary the distances between the two relays with $L_{12} =$ 200 m/300 m. Within the increase of distance between relays, the distances of source–relay and relay–destination links also increase, leading to a slow growth of the maximal rate for scenario A. Meanwhile, for B, due to the loss of modulation degree, the symbol error rate is high, even when the IRI is completely canceled and the packet rates are still maintained at a small level. However, the CFNC-based IRI response still significantly outperforms the other models.

Subsequently, we fix $L_{12} = 200$ m and change the distance of source–relay and relay–destination links. In Fig. 4, "Case 1" denotes the scenario that the relays are closer to the source node than the destination. In "Case 2," the relays are located near the destination. It can be seen from Figs. 2 and 3 that, when the maximal packet rates are achieved, the source always has larger transmit power than that of relays. This is due to the fact that large transmit power of the source is necessary to combat the IRI. In Fig. 4, for scenario A or C, when

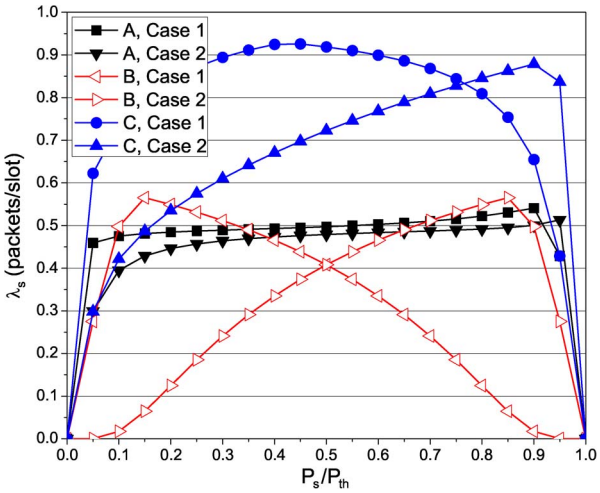

Fig. 4. Achievable packet rates with different locations of relays.

relays are close to the source, owing to short-distance transmissions, it requires less power to be assigned to the source when achieving the same $S-R_i$ performance as those in previous simulations. As a result, the maximal achievable packet rate of Case 1 is larger than that of Case 2. For scenario B, its performance is only determined by $\min\{\mu_{si}, \mu_{id}\}$. Thus, whether the relays are close to the source or the destination will not affect the results. This figure provides significant insights into relay selections, i.e., those relays that are close to the source node have higher priority to be selected as cooperation partners.

V. Conclusion

In this paper, we have proposed a cross-layer model for DF two-path relay networks, introducing stable throughput analysis. Together with the outage probabilities derived in the physical layer, the stable throughput region was presented. Subsequently, we introduced a power-allocation scheme to maximize the achievable packet rate at the source node subjected to queue stabilities and power constraint. The results play a significant role in determining whether cooperation can satisfy the QoS requirement (data rate) and how to cooperate between the source and relays (power allocation) with a certain IRI cancellation technique. Three IRI responses were considered, and the simulation results illustrated the system behavior under various scenarios.

Appendix
Proof of Proposition 1

1) If $P^*_{s,A} + P^*_{r,A} < P_{\text{th}}$, there exists a positive real number $\alpha > 1$ that satisfies $\alpha P^*_{s,A} + \alpha P^*_{r,A} \le P_{\text{th}}$. Thus, we have $\alpha P^*_{s,A} G_{ij}/N_0 > P^*_{s,A} G_{ij}/N_0$ and $\alpha P^*_{r,A} G_{ij}/N_0 > P^*_{r,A} G_{ij}/N_0$. Meanwhile, $(\alpha P^*_s G_{ij}/\alpha P^*_r G_{12} + N_0) > (P^*_s G_{ij}/P^*_r G_{12} + N_0)$. As a result, the outage probability of each link decreases, which means that the end-to-end throughput increases. $\lambda^*_{s,A}$ is no longer the optimal solution. Thus, $P^*_{s,A} + P^*_{r,A} = P_{\text{th}}$ is verified.
2) The data arrival rates and service rates are continuously differentiable on (P_s, P_r), as are $\mu_{i,A}(P^*_{r,A}) - \lambda_{i,A}(P^*_{s,A}, P^*_{r,A})$. If $\lambda_{1,A}(P^*_{s,A}, P^*_{r,A}) < \mu_{1,A}(P^*_{r,A})$ and $\lambda_{2,A}(P^*_{s,A}, P^*_{r,A}) < \mu_{2,A}(P^*_{r,A})$, we can decrease $P^*_{r,A}$ as $\beta P^*_{r,A}$. Then, the service rates of relays decrease. Owing to continuous differentiability, there exists a β close enough to 1 that can maintain $\mu_{1,A}(P^*_{r,A}) - \lambda_{1,A}(P^*_{s,A}, P^*_{r,A}) \ge 0$ and $\mu_{1,A}(P^*_{r,A}) - \lambda_{1,A}(P^*_{s,A}, P^*_{r,A}) \ge 0$. Meanwhile, due to the lower transmit power of relays, lower IRI can be obtained. Thus, the service rates of the source node also increase, leading to a larger achievable packet arrival rate than $\lambda^*_{s,A}$, contradicting the assumption. Thus, the second property is proved.

References

[1] J. N. Laneman, D. N. C. Tse, and G. W. Wornell, "Cooperative diversity in wireless networks: Efficient protocols and outage behavior," *IEEE Trans. Inf. Theory*, vol. 50, no. 12, pp. 3062–3080, Dec. 2004.
[2] Y. Fan, C. Wang, J. S. Thompson, and H. V. Poor, "Recovering multiplexing loss through successive relaying using repetition coding," *IEEE Trans. Wireless Commun.*, vol. 6, no. 12, pp. 4484–4493, Dec. 2007.
[3] H. Wicaksana, S. Ting, C. Ho, W. Chin, and Y. Guan, "AF two-path half duplex relaying with inter-relay self interference cancellation: Diversity analysis and its improvement," *IEEE Trans. Wireless Commun.*, vol. 8, no. 9, pp. 4720–4729, Sep. 2009.
[4] C. Luo, Y. Gong, and F.-C. Zheng, "Full interference cancellation for two-path relay cooperative networks," *IEEE Trans. Veh. Technol.*, vol. 60, no. 1, pp. 343–347, Jan. 2011.
[5] L. Sun, T. Zhang, and H. Niu, "Inter-relay interference in two-path digital relaying systems: Detrimental or beneficial?" *IEEE Trans. Wireless Commun.*, vol. 10, no. 8, pp. 2468–2473, Aug. 2011.
[6] Y. Gong, C. Luo, and Z. Chen, "Two-path succussive relaying with hybrid demodulate and forward," *IEEE Trans. Veh. Technol.*, vol. 61, no. 5, pp. 2044–2053, Jun. 2012.
[7] Y. Ji, C. Hao, A. Wang, and H. Shi, "Partial inter-relay interference cancellation in two path successive relay network," *IEEE Commun. Lett.*, vol. 18, no. 3, pp. 451–454, Mar. 2014.
[8] H. Lu, P. Hong, and K. Xue, "High-throughput cooperative communication with interference cancellation for two-path relay in multi-source system," *IEEE Trans. Wireless Commun.*, vol. 12, no. 10, pp. 4840–4851, Oct. 2013.
[9] H. Lu, P. Hong, and K. Xue, "Generalized inter-relay interference cancellation for two-path successive relaying systems," *IEEE Trans. Veh. Technol.*, vol. 63, no. 8, pp. 4113–4118, Oct. 2014.
[10] B. Rong and A. Ephremides, "Cooperative access in wireless networks: Stable throughput and delay," *IEEE Trans. Inf. Theory*, vol. 58, no. 9, pp. 5890–5907, Sep. 2012.
[11] A. Fanous and A. Ephremides, "Stable throughput in a cognitive wireless network," *IEEE J. Sel. Areas Commun.*, vol. 31, no. 3, pp. 523–533, Mar. 2013.
[12] C.-C. Chu, H.-C. Wang, and C.-L. Wang, "Suboptimal power allocation for a two-path successive relay system with full interference cancellation," in *Proc. IEEE VTC Spring*, Yokohama, Japan, May 2012, pp. 1–5.
[13] R. Loynes, "The stability of a queue with non-interdependent interarrival and service times," *Proc. Cambridge Philos. Soc.*, vol. 58, no. 3, pp. 497–520, 1962.
[14] D. Bertsekas and R. Gallager, *Data Networks*, 2nd ed. Englewood Cliffs, NJ, USA: Prentice-Hall, 1987.
[15] S. M. Selby, Ed., *CRC Standard of Mathematics Tables*. Cleveland, OH, USA: Chemical Rubber, 1973.
[16] *Radio Frequency (RF) System Scenarios*, Third-Generation Partnership Project, Sophia Antipolis Cedex, France, TR 36.942, v9.0.1, Dec. 2010.